Electromechanics & MEMS

Academic and Research Staff
Professor Jeffrey H. Lang

Visiting Scientists and Research Affiliates
Dr. Padraig Cantillon-Murphy

Graduate Students
William Bosworth, Samuel Chang, Vicente Fernandez, Stephen Hou, David Jenicek, Zachary Trimble, Frank Yaul

Technical and Support Staff
Dimonika Bray

Research Themes

The work reported here combines elements of electromechanics, power electronics and applied control primarily in the analysis, design and control of energy conversion systems. The principal applications focus on systems involving: macro-scale rotating machinery; micro-scale (MEMS) sensors, actuators and energy converters; and flexible structures. In these applications, the dual use of electromechanical actuators as motion and force sensors, and vice versa, is also a common theme.

1. Energy Harvesting for Hybrid Insect MEMS

Sponsor
DARPA, Air Force Research Laboratory

Project Staff
Samuel Chang, David Otten, Frank Yaul

Overview

This project is part of the "DARPA Hybrid Insect MEMS" (HIMEMS) Program. The objective of that program is to develop a functioning command and control interface between the neurological and behavioral systems of an insect, and electronics implanted in that insect. To that end, each participating group in the program is challenged to direct its chosen insect to crawl or fly from one location to the next on wireless command, over a substantial distance and extended duration. On-insect power is a significant barrier to meeting this challenge. Correspondingly, the objective of this project is to provide the required on-insect power, near 1 mW, through vibration energy harvesting. The remainder of our group, comprising other faculty from MIT and the Universities of Arizona and Washington, and their staff and students, work on other aspects of meeting the challenge.

The insect chosen here is *manduca sexta*, the hawkmoth, and energy harvesting during its flight is based on wing-beat body vibrations. These are narrow-band vibrations of ±1 mm near 25 Hz, measured normal to the dorsal surface. The dorsal payload volume for carrying a harvester is tent shaped, with a 6-8 mm base, and a 10-15 mm height beneath the wings at the apex of their flapping motion. The length of this volume can be 4-5 cm so long as the harvester mass distribution does not affect the aerodynamic balance of the moth. The payload capacity of *manduca sexta* is about 1 g. The mass of the energy harvester should be less to accommodate additional payloads, some to be powered by the harvester.

The narrow bandwidth of the moth body vibrations argues for a resonant energy harvester employing a spring and proof mass to enhance the vibration stroke; a stroke near ±7 mm is allowed beneath the moth

wings at the apex of their motion. To provide a 1-mW output power at 25 Hz then requires the conversion of 40 μJ during each cycle with a peak force of 3.6 mN, assuming zero reactive mechanical power and 100% energy-conversion efficiency from the harvester. This is incompatible with small low-mass low-voltage capacitive or piezoelectric energy conversion, and so a magnetic energy harvester is used here. Correspondingly, energy harvesting is implemented in two steps. The first step involves a reciprocating energy converter that is a linear AC poly-phase permanent-magnet synchronous generator. The generator is supported by a resonant spring-mass structure that enhances the moth body vibrations; the generator magnets and cores serve as the resonating mass. During the second step, power electronics rectify and condition the AC output from the generator for general-purpose use at 1 VDC.

As shown in Figure 1, the resonant energy converter comprises a support structure, moving magnets and core, and stationary windings. The first three components form a spring-mass resonator tuned to the wing-beat frequency of the moth; the structure is the spring, and the magnets and core provide the dominant proof mass. The spring is folded so as to be compact, and the structure/spring is printed from acrylonitrile butadiene styrene (ABS) plastic to minimize mass. The bending of the folded spring can be seen in Figure 1, which also shows the components of an energy harvester under test on a vibration table. The magnets, core and windings form a linear thee-phase AC permanent-magnet synchronous generator. The stationary windings are fabricated from two stacked two-layer printed circuit boards that stand vertically in the center of the energy harvester. Together they form a three-phase star-connected stator with two poles per phase. Wrapped around the windings is a box-shaped structure that supports the moving magnets and cores on both sides. The magnets are hidden from view, but the cores extend slightly above and below, and so one is partly visible on the near side of the windings. The three-pole magnetic flux from the magnets and core is horizontal, cutting through the winding poles.

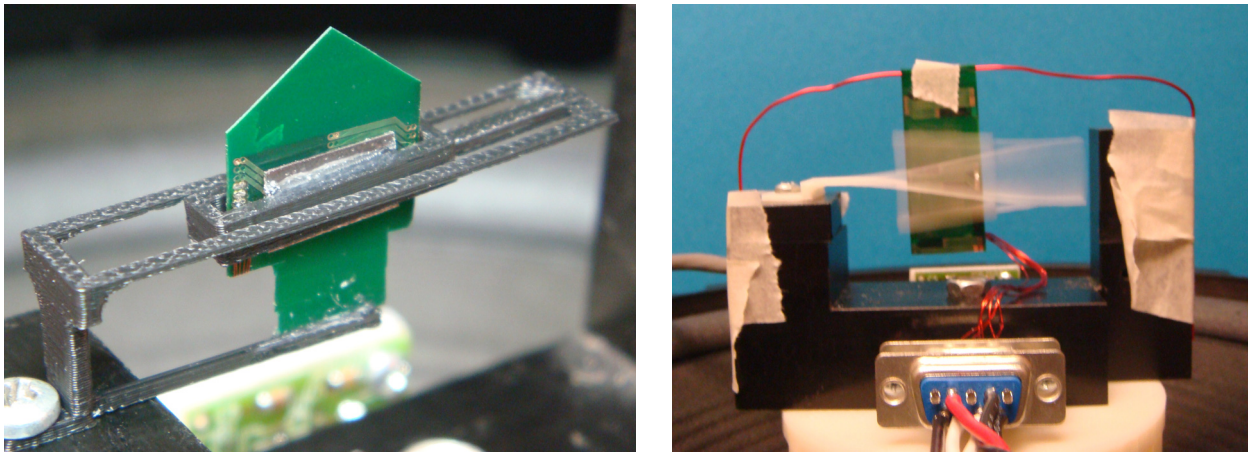

Figure 1: close-up view of an energy converter (left) and its component testing on a shaker table (right).

As shown in Figure 2, the power electronics within the energy harvester operate to extract maximum power from the poly-phase AC generator, and deliver that power to a 1-VDC load, through two stages. The first stage is a combined AC/DC synchronous rectifier and DC/DC boost converter. There is one such stage for each generator phase, and the outputs of the three parallel stages deliver energy to a common intermediate energy storage capacitor at about 50 mV. Following the capacitor is a single DC/DC boost converter that raises the voltage from 50 mV to 1 V. To deliver maximum power to the load, each first stage shuts down when its input voltage magnitude falls below 10 mV; below a 10-mV input the power electronics consume more power than they extract.

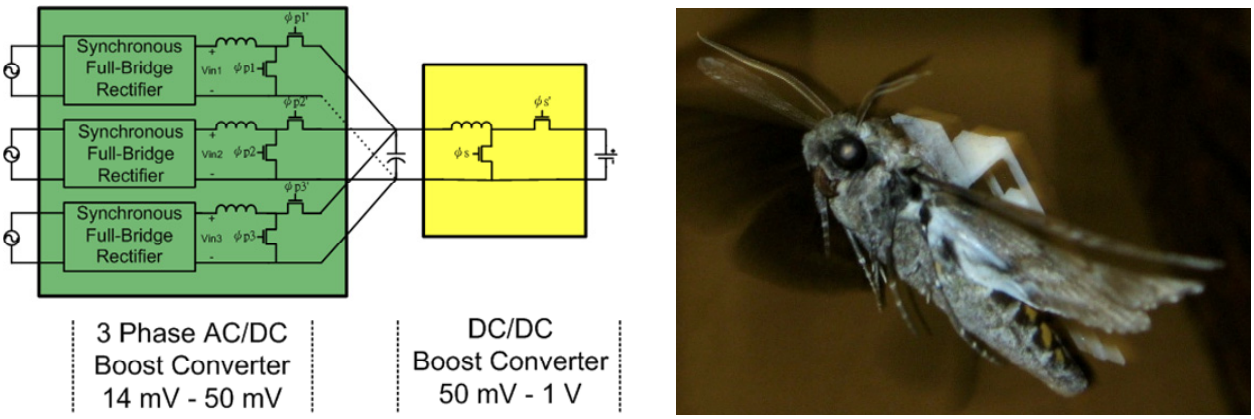

Figure 2: a block diagram of the power electronics (left), and an energy harvester on a moth in flight (right).

The components of the energy harvester have been tested using the shaker table shown in Figure 1. An early energy converter similar to those shown in Figures 1 and 2 exhibited a mass of 1.28 g, and produced a 1.7-mW output power when shaken with an amplitude of only ±0.37 mm at 25.8 Hz. In this case the resulting generator amplitude was ±7.82 mm. Work is now underway to reduce the mass of the energy converter. A discrete version of the power electronics has also been simultaneously tested, demonstrating 70% efficiency, and yielding an output power of 1.2 mW. It is estimated that the mass of an integrated version would be near 40 mg, exclusive of inductors. Work is now underway to develop an integrated implementation of the power electronics while simultaneously improving its efficiency and making use of the natural inductance of the generator in the first-stage DC/DC converter.

Further details may be found in [1,2].

2. Touch at a Distance: Pressure Sensor Arrays for Passive Underwater Navigation

Sponsors
Sea Grant, Singapore-MIT Alliance for Research and Teaching

Project Staff
Vicente Fernandez, Franz Hover (MIT Mechanical Engineering Faculty), Stephen Hou, Michael Triantafyllou (MIT Mechanical Engineering Faculty), Frank Yaul

Overview

Inspired by the lateral-line organ in fish, the objective of this project is the development of a passive system for autonomous underwater vehicles (AUVs) that can detect, classify and locate underwater objects. The lateral line sensory organ in fish enables some species to form three-dimensional maps of their surroundings. The canal subsystem of the organ acts as an array of pressure sensors. Interpreting the spatial pressure gradients allows fish to perform a variety of actions, from schooling, to tracking prey, to recognizing nearby objects. Similarly, by measuring pressure variations on a vehicle surface, an engineered dense pressure-sensor array could enable the identification and location of obstacles during navigation. Such a system consumes little power, and has advantages over visual and sonar navigation in murky and cluttered surf zones. Our navigation system is based upon two key technologies: (1) large arrays of very small pressure sensors that can be mounted on the surface of an AUV, and (2) the pressure signal processing algorithms through which object detection, classification and location is implemented.

The specifications for the individual pressure sensors in an array are derived from our experience with classifying objects using pressure signals measured with off-the-shelf sensors. In particular, it appears necessary to sense differential pressures along the array having a dynamic range of several thousand Pa, with a resolution of 10 Pa or better, and a bandwidth of at least several hundred Hertz. A space between sensors on the order of several millimeters or less is also desirable. Pressure sensors designed and fabricated following the principles of Micro Electromechanical Systems (MEMS) appear capable of meeting these specifications, and so this is the development path taken here.

We are now pursuing in parallel two different approaches to the development of arrays of tens to hundreds of MEMS pressures sensors meeting the above specifications. The first approach employs strain gauges mounted on flexible diaphragms. As the pressure outside a sensor varies, its diaphragm deflects, and its strain gauges detect the deflection. At present, these arrays are being developed in silicon for convenience. In the future they will be transferred to a more flexible substrate, making them suitable for use in AUV applications. The second approach makes use of metal-doped conducting polymers. As this material is compressed, it undergoes a change in resistivity up to ten orders of magnitude, enabling the detection of small pressure changes. Since the material is flexible, it is already a good candidate for use in AUV applications.

The pressure sensors employing flexible diaphragms and strain gauges are now capable of meeting the required specifications. We are now in the process of completing detailed characterizations of their performance, and the performance of their attendant external electronic amplifiers. Figure 3 shows a photograph of a pressure sensor array wafer mounted in a plexiglass frame for underwater testing. The characterization is in preparation for the fabrication of a new generation of sensor arrays with fully-integrated internal amplifiers. The integrated amplifiers will help improve signal-to-noise ratios. More importantly, these amplifiers will also enable a matrix sensor addressing scheme that will minimize the number of interconnects to, and simplify the pressure readout from, each sensor array.

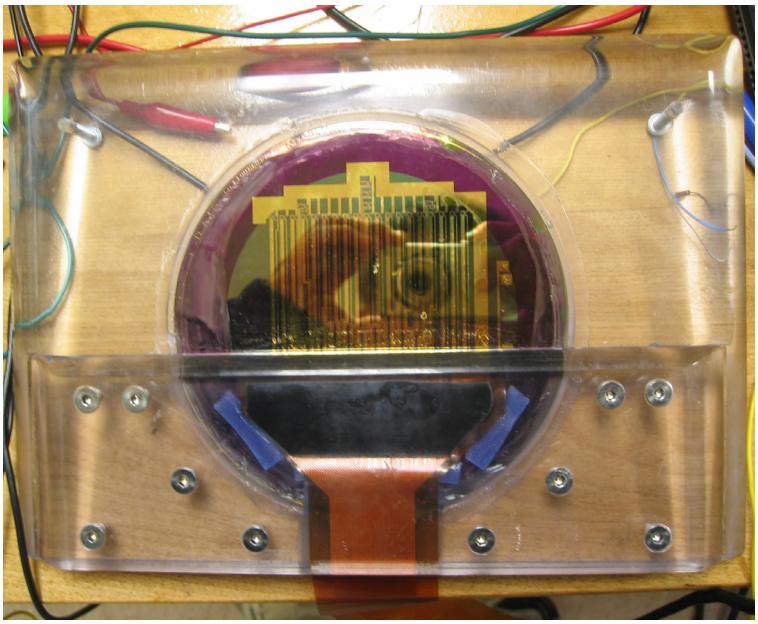

Figure 3: pressure sensor array packaged for underwater experimentation.

Our development of pressure sensors employing pressure-sensitive metal-doped conducting polymers began recently with a study of the polymers themselves. The purpose of the study was to engineer a polymer with the desired compressive mechanical response to pressure, and the desired electrical response to the resulting strain. This study has been largely completed, resulting in a satisfactory

composite material. The composite material is fabricated by mixing conductive nickel particles into an insulating silicone elastomer matrix. This mixture may be cured at room temperature, resulting in an insulating rubber-like composite. Through mechanical compression experiments we have observed that the resistance of the composite decreases smoothly and exponentially with increasing strain. A change in resistance from 10^7 ohms to 10 ohms over a 10% strain is typical. In order to maximize sensitivity to pressure, a very soft silicone with a low tensile modulus is used as the elastomer matrix. This enables a sensitivity of near 5% change in resistance per kilopascal of compressive pressure.

Experiments with fish provide evidence that they can extract from the pressure distribution along their bodies considerable practical information about nearby objects and their surroundings. In particular, the canal subsystem of the lateral line appears to be the critical component of many associated behaviors. Correspondingly, one of the key technologies under development here is a collection of algorithms that use the pressure field along a body to obtain detailed information about the presence, shape and location of objects in the nearby flow. To date, these algorithms are tested using pressure signals collected in a towing tank using small arrays of commercial off-the-shelf pressure sensors.

One important set of algorithms tracks vortices. Vortices are shed by all objects as they propel themselves through a fluid, and hence are indicators of important objects. One set of experiments demonstrated that a Kalman Filter based on the model of a single vortex in potential flow near a wall tracked an actual vortex reasonably well; the wall modeled the body that enclosed the pressure sensor array. Here, the vortex was generated by a foil stroke. Since the early experiments, the filter has been improved to include the second vortex that must be generated by the foil stroke. Additionally, experiments showed that, due to the actual rounded tubular shape of the sensor, there was negligible interaction between the vortex pair and the sensor body. In view of the two-dimensional potential flow approximation upon which the filter was based, it appeared to be more accurate to ignore the presence of the sensor body than to include a wall. Consequently, the Kalman Filter model was expanded to include two vortices, but the vortex strengths were assumed to be opposite in sign and equal in magnitude. This resulted in substantial improvements to the speed of convergence of the tracking estimate, and to the accuracy of the estimate in comparison to particle-image-velocimetry measurements of fluid motion.

A second pair of algorithms was developed to detect the presence of vertical cylinders moving through the water past the pressure sensor array. The first algorithm used a linear classifier to identify the cylinder on the basis of several pre-selected features in the pressure signals. This algorithm worked reasonably well, but exhibited a misclassification rate of just under 10%. The second algorithm again used a linear classifier. This time, however, Principal Component Analysis was used to select the features with which to perform classification. In this case, the results were considerably better, yielding a 1% misclassification rate. These experiments indicate that it is possible to reliably identify and classify underwater objects using pressure measurements taken with a pressure sensor array.

Further details may be found in [3,4,5].

3. High-Performance Heat Exchangers for Electronic Systems

Sponsor
DARPA

Project Staff
John Brisson (Mechanical Engineering Faculty), David Jenicek, Evelyn Wang (Mechanical Engineering Faculty)

Overview

This project is part of the “DARPA Microtechnologies for Air-Cooled Exchangers” (MACE) Program. The objective of The MACE Program is to develop advanced heat exchangers for electronic systems. As a target metric, such heat exchangers should be capable of exchanging over 1000 W of input heat to

ambient air with an overall thermal resistance of less than 0.05 K/W. The exchangers may use up to 33 W of input electrical power themselves, and they must fit within a 4-inch cube, with one 4-inch-by-4-inch face of the cube serving as the heat-exchange input plane. This project is carried out in collaboration with Professors Brisson and Wang of the Mechanical Engineering Department, and their students and staff. The focus of the work reported here is on the development of an integrated blower motor for the heat exchanger.

As shown in Figure 4, the heat exchanger comprises of a complex capillary-pumped loop heat pipe with an integrated blower; the working fluid is water. The loop consists of a single evaporator layer at the bottom, and many parallel condenser layers in the middle. The evaporator layer is in contact with the heat source, and connected to the condenser layers through vertical pipes. To improve heat exchange, the stack of condenser layers is interleaved with rotating blades which force cool air down through air central duct and then radially outward across the condenser plates. A low-profile radial-flux permanent magnet synchronous motor is mounted on top and drives the rotors on a single shaft running through axially through the condenser plates and inlet air duct. The heat pipe is an important component of the system needed to create a near isothermal heat exchanger, and to minimize the overall thermal resistance. The successful operation of the heat pipe relies on efficient wicking of the water through the complex stacked geometry. Figure 5 shows a schematic of the cross-section of the heat exchanger, high-lighting the heat pipe, a schematic detailing the condenser and evaporator wicking structures.

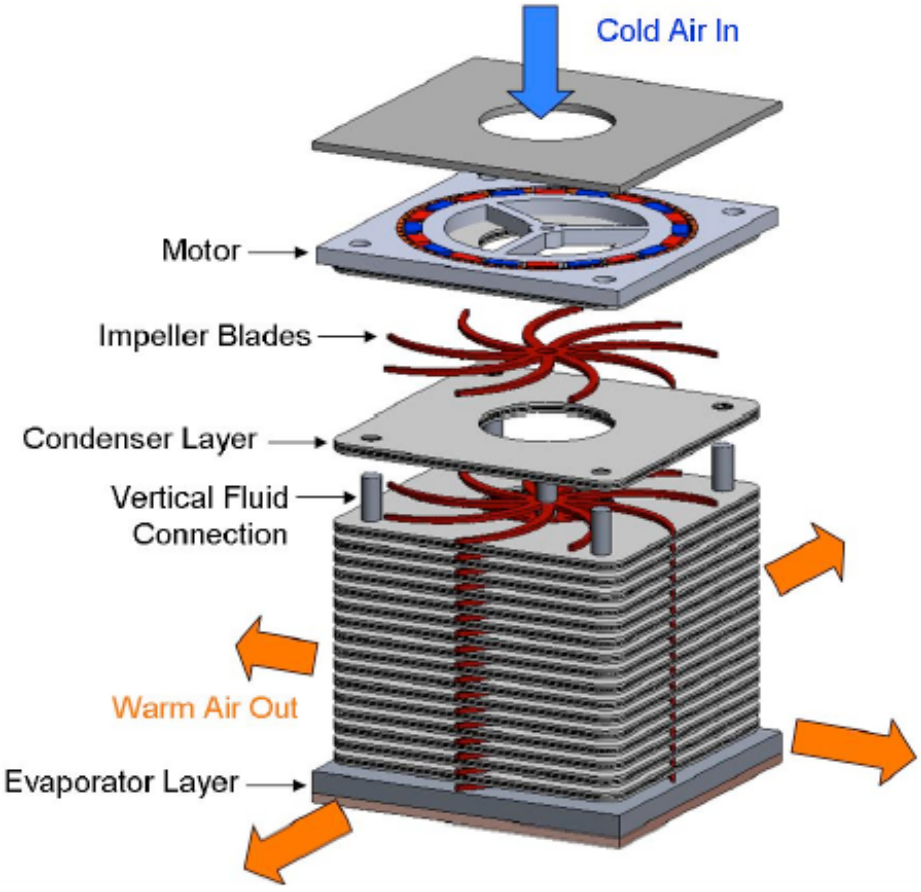

Figure 4: functional schematic of the heat exchanger.

The blowers within the heat exchanger shown in Figure 4 are driven by a low-profile permanent-magnet synchronous motor mounted on top of the exchanger. The major components of the integrated motor are shown in Figure 6. The motor is a 20-pole three-phase radial-flux motor. Its stator and rotor cores are made from magnetic steel, and it phases are wound from copper wire. It is optimized to deliver 30 W of mechanical power at 5000 rpm with a total loss of less than 3 W, including power-electronics loss.

Further details may be found in [6].

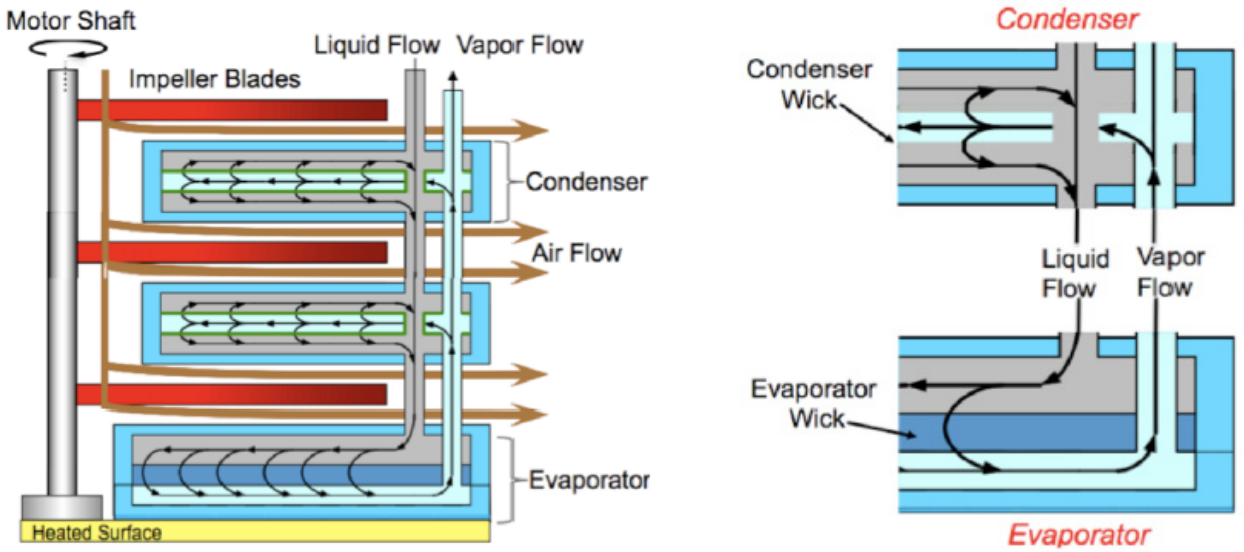

Figure 5: cross-section schematic of the integrated pump-heat sink showing the motor shaft, impeller blades, and capillary-pumped loop heat pipe (left), and schematic of the wick structures within the condenser and evaporator sections (right).

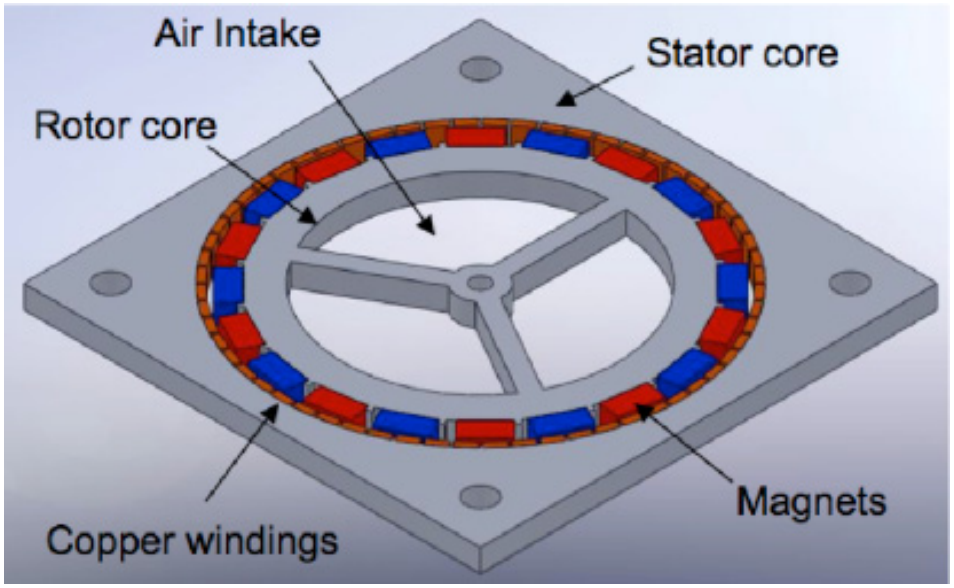

Figure 6: major components of the blower motor.

4. Self-Deploying Magnetic Devices to Assist GI Surgery

Project Staff
Padraig Cantillon-Murphy, Marvin Ryou (Brigham & Women's Hospital MD), Christopher Thomson (Brigham & Women's Hospital MD)

Overview

This project is carried out in collaboration with the Brigham & Women's Hospital of Boston, MA. Christopher Thompson, MD, and Marvin Ryou, MD, are the principal medical collaborators.

The development of natural orifice transluminal endoscopic surgery (NOTES) has generated considerable interest as a minimally-invasive alternative to traditional laparoscopic surgery. The creation of gastrointestinal-bypass anastomoses, i.e. the minimally-invasive creation of portals or channels between the stomach and intestine, for bariatric purposes or for advanced endoscopic therapies was one of the original goals of NOTES. This has since been recognized as a technically challenging proposition. Our group has designed and successfully tested a self-deploying magnetic microsystem delivered through a flexible catheter which allows for the immediate creation of bypass anastomoses via NOTES. The microsystem has been successfully tested in three live porcine studies. Pairs of mating magnetic assemblies were endoscopically deployed in the porcine stomach and jejunum before magnetically mating to provide a secure, leak-free and instantaneous access port (anastomosis) between the two organs. Immediate clinical applications of the technique are in the first step of the Roux-en-Y gastric bypass procedure for obesity and in the palliative treatment of malignant gastric outlet obstruction. This technology could also be utilized for bypass creation between any two adjacent hollow organs in the body. The benefits to the patient may include shorter hospitalization times, reduced recovery time and anesthesia, and decreased health-care costs.

The self-deploying microsystem is shown in Figure 7. It consists of four bars that deploy in a plane to form a square window. The bars are held together with hinges. The hinges between the bars eliminate the gravitational dependence observed during self-deployment in earlier designs. The bars carry embedded magnets with magnetization transverse to the plane of the window. These magnets serve two purposes. The first purpose is to cause the microstructure to deploy and lock into a square-window shape after extrusion from the laparoscope. The second purpose is to cause mating between two such windows across the seam between organs thereby initiating the formation of an anastomosis.

The hinges eliminate all but one degree of motion freedom during deployment. This allows the microstructure to be pinched closed for endoscopic delivery, and then immediately spring open to form the four-sided window upon extrusion from the endoscope. The opening mechanism is the repulsion magnetic forces (north/north or south/south) between like parallel elements in the folded position. In the folded position, there are several sources of these repulsion forces. One source is the north/north repulsion between the top face of magnets m1 and the north portion on the top face of magnets m2. Another source is the south/south repulsion between the south portion on the top face of magnets m3 and the top face of magnets m4. The final source is the complimentary repulsions (replacing north with south and vice versa) that occur via the bottoms faces of the magnets. Unlike the collection of magnets m1 and m4 which are dipolar (one sign of magnetic poles on the top face and the opposing sign of magnetic poles on the bottom face), the collection of magnets m2 and m3 are quadrapolar (two signs of magnetic poles on the top face and the opposing signs on the bottom face). The reversal in polarity in magnets m2 and m3 results in an attraction to magnets m1 and m4, respectively, during the last stage of deployment. The end result upon deployment is the four-sided assembly shown in Figure 7. The hinges and magnetization pattern make this the lowest energy state of the microstructure, guaranteeing full deployment upon extrusion from the endoscope.

Figure 8 shows a combination of laparoscopic (a,d), endoscopic (b,i,j) and fluoroscopic (c,e,f,g,h,k,l) visualization of the endoscopic deployment of two microstructures, and their subsequent mating to form an anastomosis during a live porcine study. The figure shows: (a) the initial grasping of the jejunal target with endoscopic forceps; (b) the insertion of the first magnet into the jejunum; (c) the folded first magnet

just prior to deployment in the jejunum; (d) the deployed first magnet; (e) the second magnet deploying in the stomach; (f) the second magnet after self-deployment; (g) the endoscope spearing the second magnet in the stomach; (h) mating of the first and second magnets across the gastric and jejunal walls; (i) the parent magnet after mating; (j) access to the porcine jejunum; (k) post-mating contrast agent injection; and (l) the outcome of the leak test confirming the absence of leaks from the gastrojejunostomy.

Further details may be found in [7,8,9].

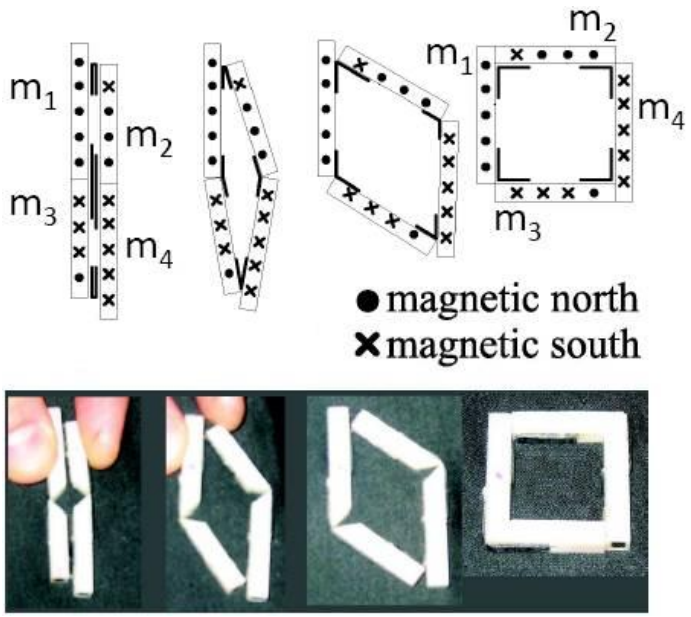

Figure 7: magnetic arrangement and self-deployment of the microsystem. The bottom sequence of figures shows the orientation of the microstructure during deployment. The top sequence of figures shows the polarity of the embedded magnets within the microstructure during the same sequence of figures.

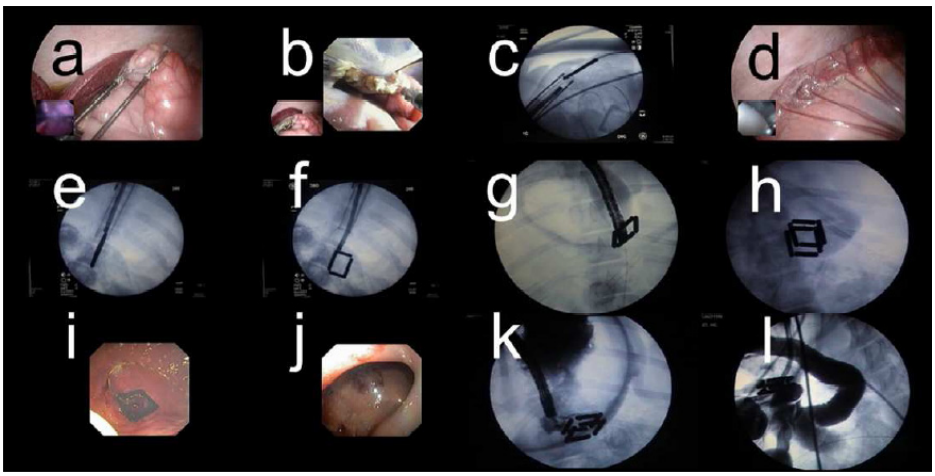

Figure 8: A combination of laparoscopic, endoscopic and fluoroscopic visualization of a live porcine study.

5. Rotational Vibration Energy Harvesting

Sponsor
Schlumberger

Project Staff
Jahir Pabon (Schlumberger Research Scientist), Alexander Slocum (MIT Mechanical Engineering Faculty), Zachary Trimble

Overview

The goal of this project is to develop an electromechanical/electronic device that can harvest energy from rotational vibrations. That energy is to be presented in electrical form for general-purpose use. The target vibrations exhibit low frequencies between 10 and 20 Hz, with acceleration amplitudes on the order of 10 rad/s^2 or less. The envelope of the harvester is constrained to a diameter of 1.25 inches and a length of 5 inches. The rotational vibrations are applied about the long cylindrical axis.

A functional diagram of the harvester electromechanics is shown in Figure 9, and a solid model is shown in Figure 10. External torsional vibrations are applied to the outer casing of the harvester around its long cylindrical axis. Within the casing is a resonant torsional spring-inertia system that couples to the strongest vibrations resulting in a relative displacement between the rotor and the casing. A single-phase permanent-magnet synchronous generator is built into the resonant system in order to transduce the rotational vibration to an electrical output thereby harvesting the input vibrational input energy. The permanent magnets are located on the suspended rotor in order to maximize the rotor inertia and hence the harvested energy. The single phase winding of the generator is surface wound on the interior of the casing, which doubles as the stator core. The power electronics that follow the electromechanics are not shown in either figure.

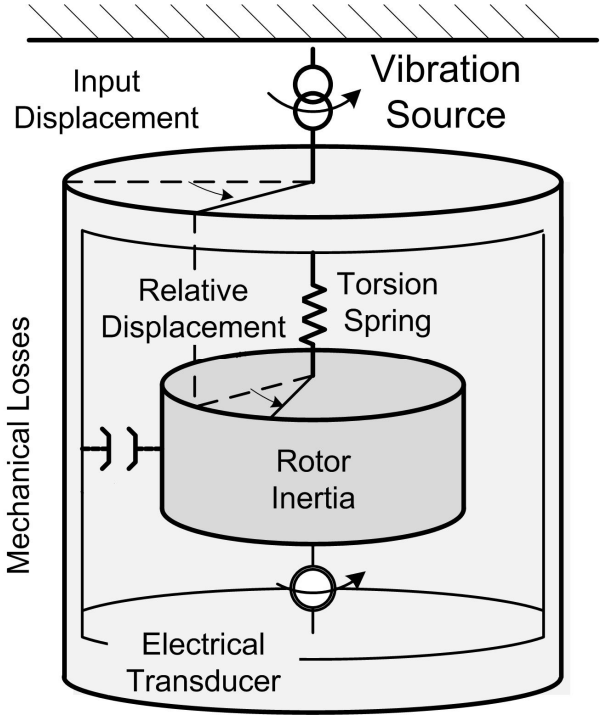

Figure 9: function diagram of the energy harvester.

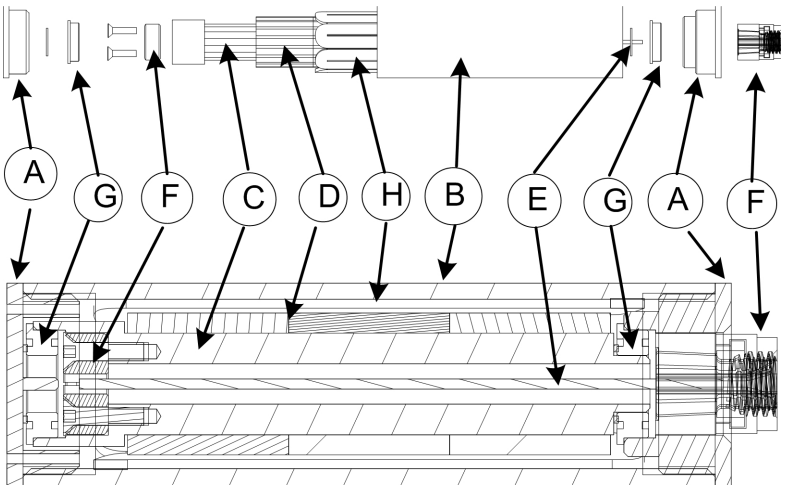

Figure 10: solid model of the energy harvester showing A - end caps and bearing supports, B – outer casing and stator core, C – rotor core, D – magnets, E - torsion rod, F - torsion rod clamps, G – bearings, and H – stator phase winding.

The harvester was tested using the vibration signal shown in Figure 11. The upper waveform in Figure 11 is a half-second segment of the vibration. The lower waveform in Figure 11 is a spectrum of the complete vibration signal. For the tests, the harvester was tuned to resonate at 18.8 Hz, corresponding to the vibration peak in Figure 11. With the vibrations show in Figure 11, the expected power out was 85 mW, and the measured power out was 74 mW. In addition, the harvester was tested with an 8 rad/s2 sinusoidal vibration at 18.8 Hz. The expected power was 220 mW, and the measured power out was 205 mW.

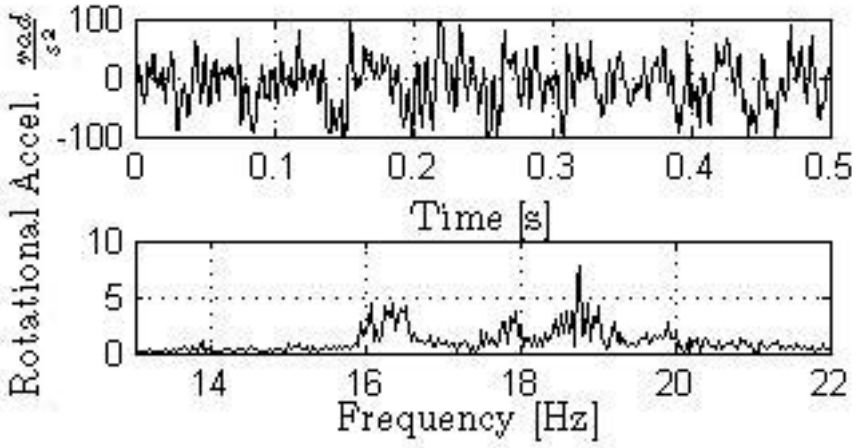

Figure 11: input vibration in the form of a time signal (above) and a frequency spectrum (below).

As part of the test procedure the design model for the harvester was used to predict the voltage output from its generator under matched load when driven by the vibrations in Figure 12; this voltage was compared to the measured voltage with the same load. The results are shown in Figure 12. The good match between experiment and theory validate the design model.

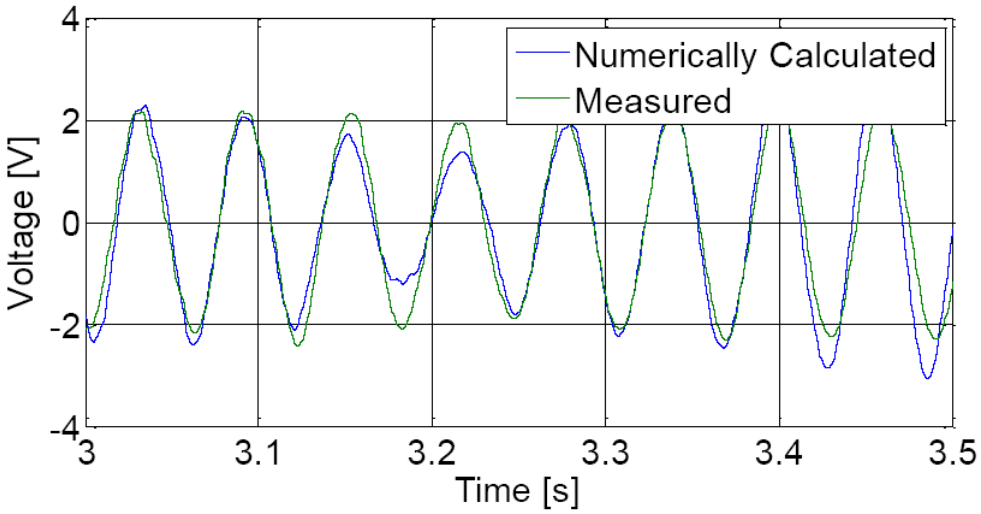

Figure 12: predicted (numerically calculated) and measured generator voltage with a matched load under excitation by the vibrations shown in Figure 11.

Future development will focus on the adaptive tuning of the energy harvester so that it can track the spring-inertia resonance frequency that results in the maximized harvested energy.

6. Sand Control in Oil Wells

Sponsors
Schlumberger

Project Staff
William Bosworth, Julio Guerrero (Schlumberger Research Scientist)

Overview

A large percentage of future oil wells will be deeper and more predisposed to producing sand than those drilled today. This will affect worldwide oil production in the near future. Sand produced down hole erodes hardware, blocks tubules, and creates down-hole cavities. Sand must also be separated and disposed of on the surface. Current well completion methods that allow sand-prone reservoirs to be exploited can severely reduce production efficiency. A significant challenge, then, is to complete an oil well while keeping formation sand in place without unduly restricting productivity, and to prevent sand from forming during oil-well operation. In response, this project seeks to develop electromechanical actuators for sand control during oil-well exploration and operation. Examples include electromechanical systems that exert a load on the formation.

Publications

[1] S. C. Chang, F. M. Yaul, A. Dominguez-Garcia, F. O'Sullivan, D. M. Otten and J. H. Lang; ”Harvesting energy from moth vibrations during flight"; Proceedings: PowerMEMS Workshop, 57-60, Washington DC, December 1-4, 2009.

[2] S. C. Chang; “A 1-mW Vibration Energy Harvesting System for Moth Flight-Control Applications”; SM Thesis, MIT EECS Department, February 2010.

[3] V. I. Fernandez, S. M. Hou, F. S. Hover, J. H. Lang and M. S. Triantafyllou; "MEMS-array pressure sensing for underwater navigation"; Proceedings: Undersea Distributed Network Systems Conference, Newport, RI, February 13-15, 2007.

[4] V. I. Fernandez, S. M. Hou, F. S. Hover, J. H. Lang and M. S. Triantafyllou; "Lateral line inspired MEMS-array pressure sensing for passive underwater navigation"; Proceedings: Unmanned Untethered Submersible Technology Symposium, Sensors Paper #4, Durham, NH, August 19-22, 2007.

[5] V. I. Fernandez, S. M. Hou, F. S. Hover, J. H. Lang and M. S. Triantafyllou; "Development and application of distributed MEMS pressure sensor array for AUV object avoidance"; Proceedings: Unmanned Untethered Submersible Technology Symposium, Sensors Paper #A.1, Durham, NH, August 24-26, 2009

[6] M. McCarthy, J. Allison, D. Jenicek, A. Kariya, C. Koveal, J. H. Lang, J. G. Brisson and E. N. Wang; ``High-performance air-cooled heat exchanger with an integrated capillary-pumped loop heat pipe''; Proceedings: Twelfth Intersociety Conference on Thermo and Thermomechanical Phenomena in Electrical Systems, Las Vegas, NV, June 2-5, 2010.

[7] M. K. Ryou, P. Cantillon-Murphy, J. H. Lang and C. C. Thompson; ``Transoral endoscopic creation of immediate cholecysto-gastrostomy using smart self-assembling magnets via endoscopic needle (SAMSEN)"; Gastrointestinal Endoscopy, 71, AB242, April 2010. Also presented at Digestive Disease Week, New Orleans, LA, May 1-5, 2010.

[8] M. K. Ryou, P. Cantillon-Murphy, D. E. Azagury, S. N. Shaikh, G. Ha, J. H. Lang, and C. C. Thompson; “Transoral endoscopic creation of immediate gastrojejunostomy using self-assembling magnets via endoscopic needle (SAMSEN)”; Gastroenterology, May 2010. Also presented at Digestive Disease Week, New Orleans, LA, May 1-5, 2010.

[9] M. K. Ryou, P. Cantillon-Murphy, S. Shaikh, D. Azagury, G. Ha, J. H. Lang and C. C. Thompson; ”Harnessing the power of magnets: novel uses in advanced endoscopic therapies"; American Society of Gastrointestinal Endoscopy Video Forum, New Orleans, LA, May 3, 2010.